Biomass Chars: The Effects of Pyrolysis Conditions on Their Morphology, Structure, Chemical Properties and Reactivity

Chamseddine Guizani, Mejdi Jeguirim, Sylvie Valin, Lionel Limousy, Sylvain Salvador

energies

MDPI

Article

Biomass Chars: The Effects of Pyrolysis Conditions on Their Morphology, Structure, Chemical Properties and Reactivity

Chamseddine Guizani [1], Mejdi Jeguirim [2,*], Sylvie Valin [3], Lionel Limousy [2] and Sylvain Salvador [4]

1 University Grenoble Alpes, CNRS, Grenoble INP, LGP2, F-38000 Grenoble, France; chamseddine.guizani@lgp2.grenoble-inp.fr
2 Institut de Sciences des Matériaux de Mulhouse, UMR CNRS 7361, 15 rue Jean Starcky, 68057 Mulhouse, France; Lionel.limousy@uha.fr
3 CEA, LITEN/DTBH/SBRT/LTB, 38054 Grenoble CEDEX 09, France; Sylvie.valin@cea.fr
4 RAPSODEE, Mines Albi, CNRS UMR 5302, Route de Teillet, 81013 ALBI CT CEDEX 09, France; sylvain.salvador@mines-albi.fr
* Correspondence: mejdi.jeguirim@uha.fr; Tel.: +33-389-608-661

Academic Editor: Shusheng Pang
Received: 12 April 2017; Accepted: 6 June 2017; Published: 11 June 2017

Abstract: Solid char is a product of biomass pyrolysis. It contains a high proportion of carbon, and lower contents of H, O and minerals. This char can have different valorization pathways such as combustion for heat and power, gasification for Syngas production, activation for adsorption applications, or use as a soil amendment. The optimal recovery pathway of the char depends highly on its physical and chemical characteristics. In this study, different chars were prepared from beech wood particles under various pyrolysis operating conditions in an entrained flow reactor (500–1400 °C). Their structural, morphological, surface chemistry properties, as well as their chemical compositions, were determined using different analytical techniques, including elementary analysis, Scanning Electronic Microscopy (SEM) coupled with an energy dispersive X-ray spectrometer (EDX), Fourier Transform Infra-Red spectroscopy (FTIR), and Raman Spectroscopy. The biomass char reactivity was evaluated in air using thermogravimetric analysis (TGA). The yield, chemical composition, surface chemistry, structure, morphology and reactivity of the chars were highly affected by the pyrolysis temperature. In addition, some of these properties related to the char structure and chemical composition were found to be correlated to the char reactivity.

Keywords: biomass; pyrolysis; entrained flow reactor; char characterization

1. Introduction

Economic and environmental issues related to the non-avoidable depletion of fossil fuels are urging governments all over the world to modify their strategies, and shift from a fossil-fuel-based economy to a bio-resources-based one. Hence, bio-refining biomass instead of petroleum to obtain energy and high added-value products represents a major challenge for a sustainable future [1].

In a bio-refinery, the biomass can be transformed into a variety of bio-based products such as biofuels and bio-based chemicals and materials, just as in fossil fuel refineries. Energy can also be obtained from biomass processing for the production of heat and electricity [2].

Different processes exist that allow the transformation of raw biomass into desirable bio-based products and/or energy. For instance, biomass pyrolysis, which is a thermochemical process, has the advantage of transforming the raw material after heating in the absence of oxygen into bio-oil, gas and char that can be valorized separately [3]. The proportion of these three products depends

strongly on the pyrolysis conditions; namely, reactor temperature and heating rate. Low temperatures (<600 °C) favor the production of bio-oil and bio-char while high temperatures (>600 °C) maximize the production of gas. At relatively low temperatures, a fast heating rate is desirable to maximize the bio-oil yield.

As mentioned previously, the pyrolysis products may be valorized in different applications. The bio-oil can be used as a fuel for heating, or for the production of chemicals [4]. Gas can be energetically valorized into heat/electricity or further processed to produce biofuels. Depending on its quality, the solid bio-char can be gasified [5], used for the production of activated carbons [6], for the production of graphene [7], or for soil remediation [8].

The reactivity and physicochemical properties of the char are crucial for selecting the suitable valorization pathway. The pyrolysis process highly affects the physicochemical properties of the residual char as well as its reactivity. Indeed, the reactor temperature, the particle heating rate and residence time in the reactor directly influence the char yield and properties. In particular, the char chemical composition depends on the pyrolysis temperature [9]. As temperature increases, O and H atoms are released in the gas phase due to the pyrolysis of biomass components and cracking of the residual char. Moreover, some minerals are volatilized and the solid char becomes richer in carbon [10–12].

The char texture and structural organization change over the pyrolysis reaction due to the thermal degradation of the major biomass components; namely, cellulose, hemicellulose and lignin [13]. The structural features and surface chemistry of the bio-chars are affected by the pyrolysis temperature and residence time. Surface functionality decreases as temperature increases due to biomass pyrolysis and char cracking reactions [14]. Char structure gets more organized when increasing the temperature and residence time in the reactor, and tends towards a graphite-like structure [15–17].

Other studies reported results on the evolution of the yield and above-mentioned physical and chemical characteristics of bio-chars upon fast and slow pyrolysis and correlated them to the pyrolysis experimental conditions such as temperature and heating rate [18,19]. For instance, in [18], the authors found that the char yield decreased when increasing the heating rate up to a value of 600 °C/s, above which the char yield was constant. In [19], the authors analyzed chars coming from slow and fast pyrolysis as well as gasification processes. They observed a pronounced decrease in aromatic C-H functionality between slow pyrolysis and gasification chars using Nuclear Magnetic Resonance (NMR) and Fourier Transform Infrared-Photoacoustic (FTIR-PAS) Spectroscopies. Moreover, NMR estimates of fused aromatic ring cluster size showed fast and slow pyrolysis chars to be similar (7–8 rings per cluster), while higher- temperature gasification char was much more condensed (17 rings per cluster).

Analyzing the char structural evolution upon heat treatment, McDonald-Wharry et al. [15] observed that the IV/IG Raman structural ratio was correlated with heat treatment temperature for various types of chars. Morin et al. observed a decrease of beech char reactivity with an increasing pyrolysis temperature [20]. Other authors also correlated several char properties, especially those relating structural parameters of the char and their reactivities [21,22].

In the present work, beech wood pyrolysis experiments were performed in an entrained flow reactor (EFR) at between 500 °C and 1400 °C for different gas residence times. These experimental conditions were wide enough to obtain chars with various properties. The recovered chars were characterized in terms of their morphological, structural, surface chemistry properties as well as their reactivity towards oxygen. Correlations between the different char properties were identified. Such correlations could be helpful for developing a preliminary understanding of char properties, and therefore for identifying their potential valorization pathways.

2. Materials and Methods

2.1. Raw Biomass

The raw biomass used in this work is beech wood supplied by the Sowood company. The raw wood is finely ground with particles having sizes ranging from tens of microns to a few millimeters. After sieving, particles having a mean size of 370 µm were selected for the pyrolysis experiments. This mean size should be appropriate to avoid heat and mass transfer limitations during the EFR pyrolysis experiments.

The moisture content was determined by drying at 105 °C according to the NF-EN-14774 standard. Ash content was determined by burning the sample in air at 850 °C according to the NF-EN-14775 standard. The oxygen content was determined by difference to the sum of C, H, N and ash contents. The proximate and ultimate analyses are shown in Table 1.

Table 1. Proximate and ultimate analyses of beech wood.

Proximate Analysis	Value
Moisture [wt % ar *]	8.7
Volatile Matter [wt % db **]	84.3
Fixed carbon [wt % db]	15.2
Ash (815 °C) [wt % db]	0.5
Ultimate analysis [wt % db]	
C	49.1
H	5.7
N	0.15
S	0.045
O (by difference)	44.5

* ar: as received; ** db: dry basis.

2.2. Experimental EFR Set Up

The EFR experimental set-up was previously described in detail by Billaud et al. [23]. It consists of an alumina tube inserted in a vertical electrical heater with three independent heating zones. The dimensions of the tube are 2.3 m in length and 0.075 m in internal diameter. The heated zone is 1.2 m long. The temperature along the heated zone is homogeneous and verified prior to the experiment by moving a thermocouple vertically along this zone. The temperature profile is assumed to be the same during the experiment, as it is not possible to monitor it along the z axis while injecting biomass and collecting the products. The EFR works at atmospheric pressure and can reach a maximum temperature of 1400 °C. The wood particles are continuously fed into the reactor using a gravimetric feeding system. The main N_2 gas stream is electrically pre-heated before entering the reactor. A sampling probe allows collection of the gas produced, which is analyzed by a gas chromatograph. The remaining solid falls by gravity in a settling box. Tars are condensed in a cold trap, while soot is collected by a filter, and is weighed after the reaction to determine its volume.

2.3. Pyrolysis Conditions

The pyrolysis experimental conditions are summarized in Table 2. The biomass mass flow rate (1 g/min) and particle size (370 µm) were the same for all experiments. The gas residence time was controlled with the nitrogen flow rate, as the pyrolysis gas flow rate was much lower than that of the N_2. The mean gas residence time was determined knowing the nitrogen flowrate, the reactor temperature, length and cross-section.

The chars analyzed in the present work are produced from the pyrolysis of the same biomass and gathered from two experimental campaigns with two different objectives:

- The first is related to medium-temperature pyrolysis (500–600 °C), aiming at maximizing bio-oil production.
- The second concerns high-temperature pyrolysis aiming at maximizing the gas fraction [23].

For the first tests, the gas residence time was fixed at 16.6 s, while in the second tests it was fixed at 4.3 s. At high temperatures, the gas expansion induces an increase in the volumetric flow rate, lowering the residence time of gases. For practical purposes, it is not convenient to operate at lower flow rates (due to oxygen introduction in the reactor). The particle residence time (which is much more important than the gas residence time with regard to the final char characteristics) is calculated considering slip velocity between solid particles and gas. This takes into account the particle density and size, and their evolution as pyrolysis proceeds, between the density and size of wood particles and those of char particles [24]. The robustness and accuracy of the model is validated over a wide range of temperatures, atmospheres and particle sizes [23,25].

Table 2. Pyrolysis experimental conditions in the EFR.

Reactor Temperature T_{Pyr} [°C]	$\dot{m}_{biomass}$ [g/min]	Gas Residence Time [s]	Particle Residence Time t_{Res} [s]
500	1 ± 0.1	16.6 ± 0.2	2.26
550	1 ± 0.1	16.6 ± 0.2	4.03
600	1 ± 0.1	16.6 ± 0.2	5.12
800	1 ± 0.1	4.3 ± 0.1	2.33
1000	1 ± 0.1	4.3 ± 0.1	2.40
1200	1 ± 0.1	4.3 ± 0.1	2.45
1400	1 ± 0.1	4.3 ± 0.1	2.52

The particle residence time varies more at low temperatures, while it remains almost the same for temperatures above 600 °C. This is not obvious at first glance, but it has to do with the change in particle slip velocity during the pyrolysis process. At low temperatures, the pyrolysis reaction rate is not so high, and neither is the particle slip velocity. During the pyrolysis reaction, the particle slip velocity changes from that of the biomass particle to that of the char particle. The latter is much lower than the former. As the pyrolysis kinetics are slower at low temperatures, the change in particle slip velocity (from that of wood to that of char) is also slow, and consequently the residence time is also small. However, when increasing the temperature, the pyrolysis reaction accelerates, the char is formed in a shorter time inside the reactor, the slip velocity drops more rapidly to that of a char particle and, consequently, the residence time becomes higher (see the increase between 500 and 600 °C).

At higher temperatures >800 °C, the pyrolysis reaction rate is quite high and the char is formed in the first centimeters of the reactor. As it has a lower slip velocity than the biomass, it resides inside the reactor for a non-negligible period. One can see that the residence time at high temperatures is similar to that obtained at 500 °C, despite a gas velocity that is, for a time, higher at higher temperatures. As explained, this has to do with the particle slip velocity which is higher at 500 °C than at temperatures above 800 °C.

As for the 500–600 °C experiments, a large sampling probe allowing recovery of all the pyrolysis products is used. The mass of residual char is then directly weighed. The char yield is obtained by the ratio between the total mass of the residual char and the cumulated mass of the injected biomass during the pyrolysis experiment:

$$Y_{char} = \frac{m_{char}}{\int_0^{t_{end}} \dot{m}_{biomass}\, dt}$$

For all the other experiments performed above 800 °C, about 80% of the products were sampled. The char yield is then calculated using the ash tracer method, as described in detail in [24].

2.4. Characterization Techniques of the Biomass Chars

2.4.1. Proximate and Ultimate Analysis

Ash content was determined by burning the samples in air at 850 °C according to the NF-EN-14775 standard. The oxygen content was determined by difference.

2.4.2. Morphology

The morphology of the parent wood and solid residues was studied via Scanning Electron Microscopy (Philips model FEI model Quanta 400 SEM). SEM images were obtained in a high vacuum mode for both secondary electrons (topography contrast) and backscattered electrons (chemical contrast). The acceleration voltage and the electron beam spot size were carefully chosen. The solid residues were coated with a thin gold layer by using Agar automatic sputter coater prior to the observation. Energy Dispersive X-Ray analysis was also performed in order to identify the mineral species and analyze their dispersion throughout the char matrix.

2.4.3. Surface Chemistry

The surface functional groups of the solid residues were characterized using a FTIR PerkinElmer 1720 spectrometer. The FTIR spectra were recorded in the spectral range between 4000 and 500 cm^{-1} with a resolution of 4 cm^{-1} and 32 scans in attenuated total reflection (ATR) configuration.

2.4.4. Structure

The structural evolution of the chars was assessed by Raman spectroscopy. Raman spectra of the chars were recorded with a BX40 LabRam, Jobin Yvon/Horiba spectrometer. Several particles were sampled and deposited on a rectangular glass slide for the Raman analysis. Raman spectra were obtained in a backscattered configuration with an excitation laser at 635 nm. The Raman spectra at each position give an average structural information of a large number of carbon micro-crystallites. The Raman spectra were recorded at 6 locations of the char sample. The spectra were afterward analyzed using a home-made software for the background correction, normalization with G band height, average spectrum calculation, as well as different band height and integral areas measurements.

From these spectra, several parameters related to the structure were determined:

- ID: D band intensity height.
- D_{pos}: D band position.
- IG: G band intensity height.
- G_{pos}: G band position.
- IV: Valley region intensity height.
- The Total Raman Area (TRA):

$$TRA = \int_{800}^{2000} I \, d\nu \quad (1)$$

I is the intensity and $d\nu$ is the increment of the wave number.

The different band specifications and ratios are further discussed in the results and discussion section.

2.4.5. Reactivity towards Oxygen

Reactivity tests in air atmosphere were performed using the Mettler-Toledo TGA/DSC3+ thermogravimetric analyzer. The air flow rate was set at 50 mL/min. The samples were heated from 30 °C to 700 °C with a heating rate of 10 °C/min and maintained at this temperature during 1 h. The sample mass was below 5 mg to minimize heat and mass transfer limitations.

The TG oxidation experimental data were analyzed with homemade software, for smoothing, derivative calculation, derivative peak positions and values etc.

Hence, the different parameters related to the char reactivities in air were determined and can be summarized as follows:

- $\alpha = \frac{m_{(t)} - m_{(ashes)}}{m_{(0)} - m_{(ashes)}}$ is the conversion level.
- $T_{(2\%)}$ is the temperature at which $\alpha = 2\%$.
- $T_{(50\%)}$ is the temperature at which $\alpha = 50\%$.
- $T_{(98\%)}$ is the temperature at which $\alpha = 98\%$.
- $\frac{dm}{dt}_{mean} = -\frac{1}{N_{exp}} \sum_{i=1}^{N_{exp}} \left(\frac{dm}{dt}_i \right)$ is the mean reaction rate $-\frac{dm}{dt}_{max}$ is the maximum observed reaction rate.
- $T_{(peak)}$ is the temperature at the maximum reaction rate.
- $R_{mean} = -\frac{1}{N_{exp}} \sum_{i=1}^{N_{exp}} \left(\frac{dm}{dt}_i \frac{1}{m_i} \right)$ is the mean reactivity.
- $R_{index} = -\frac{1}{N_{exp}} \sum_{i=1}^{N_{exp}} \left(\frac{dm}{dt}_i \frac{1}{T_i} \right)$ is the reactivity index.

T is the temperature, $m_{(t)}$ is the char mass at time "t", $m_{(0)}$ is the initial char mass, $m_{(ashes)}$ is the mass of the residual ashes, N_{exp} is the number of experimental values.

3. Results and Discussion

3.1. Pyrolysis Product Yields

Figure 1 shows an area plot of the pyrolysis product yield distribution as a function of the reactor temperature. This area plot is drawn using the discrete values of the different yields obtained from different experimental conditions given in Table 2. Tars include the condensable species in the volatile matter and the initial moisture of the wood. At low temperatures (below 600 °C), tar and solid together represent more than 50 wt % of the products. A temperature of 500 °C maximizes the oil yield, which reaches 62.4 wt %, while the char yield is close to 14 wt %. Several investigations have mentioned 500–550 °C as the optimal temperature for maximizing the bio-oil yield during biomass pyrolysis [3]. The water content of the pyrolysis oil (tars) varied between 30% and 35% at 500 and 600 °C, respectively, which includes both moisture water and pyrolysis reaction water. The water content of the oils obtained at higher temperatures was not evaluated.

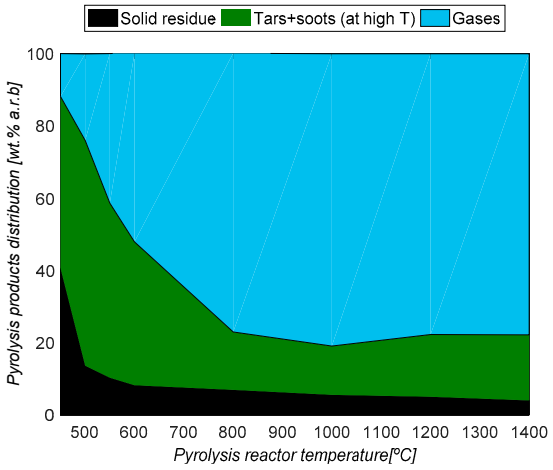

Figure 1. Pyrolysis product distribution (as received basis, a.r.b.) versus pyrolysis reactor temperature.

The production of gases increases with temperature, while that of tar and char decreases. For instance, at 800 °C, the gas yield is close to 78 wt %, while the char yield is 7%. Furthermore,

at high temperatures, the formation of soot was observed, starting from 1000 °C. A deep analysis of the operating conditions' effect on the pyrolysis product distribution can be found in previous investigations [23,26]. The main focus of the present study was to identify the effect of the operating conditions on the char characteristics.

The evolution of the char yield with the pyrolysis reactor temperature indicates two separate ranges of linear decrease: low temperatures (500–600 °C) and high temperatures (600–1400 °C). The char yield decreased from 14% to 8% between 500 °C and 600 °C (0.05%/°C, R^2 = 0.991), while it decreased from 8% to 4% between 600 °C and 1400 °C (0.005%/°C, R^2 = 0.990). The relative uncertainties in the char yields are estimated to be lower than 10%. The evolution of the char yield would be thus significant.

The lower char yield at high temperatures may be explained by several factors. Higher heating rates are known to induce lower char yields [18]. Moreover, volatile and char formation are two parallel reactions, and the latter is probably favored at higher temperatures and higher heating rates. Also, above 1000 °C, char gasification by H_2O and CO_2 is likely to consume part of the formed solid.

3.2. Microscopic Analysis of the Biochar Surfaces

In order to monitor the textural properties and the behavior of minerals on the different chars upon different pyrolysis treatment, we performed SEM analysis coupled with EDX characterization at different enlargements.

Five samples were chosen to observe the effect of the pyrolysis temperature on the surface and the properties of the biomass particles: raw biomass, and samples pyrolysed at low (500, 600 °C) and high (1200, 1400 °C) temperatures.

Figure 2 presents the surface of a particle of beech wood at different enlargements. The cell walls of the raw biomass present a homogeneous surface without any holes; the EDX analysis shows the presence of very small amounts of Ca and K, which are the main minerals present in the biomass. The elemental cartography of the surface shows that K and Ca are homogeneously dispersed inside the biomass.

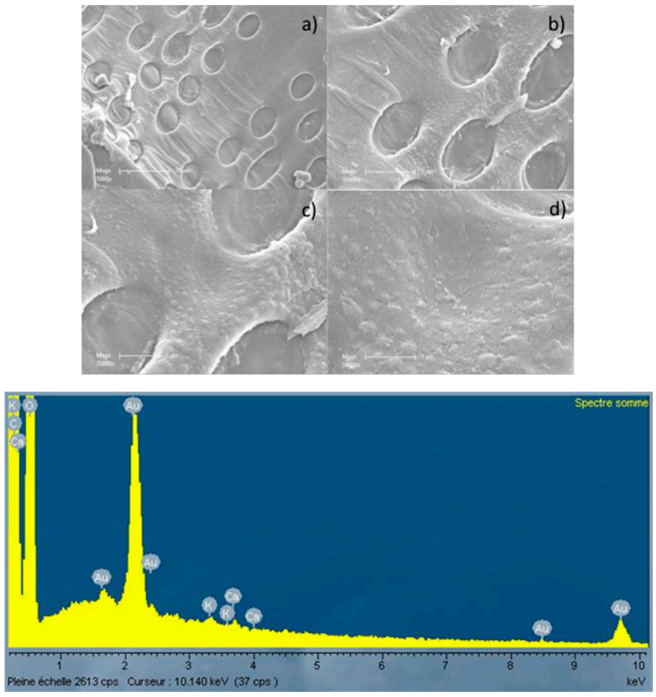

Figure 2. SEM photographs and X-ray fluorescence analysis of the surface of the raw wood particles at different enlargements (**a**) ×5000; (**b**) ×10,000; (**c**) ×20,000; and (**d**) ×50,000.

Figures 3 and 4 show the surface of the samples pyrolysed at 500 and 600 °C respectively. Different areas of the particles were observed in order to be sure that the description of these materials was representative of the materials.

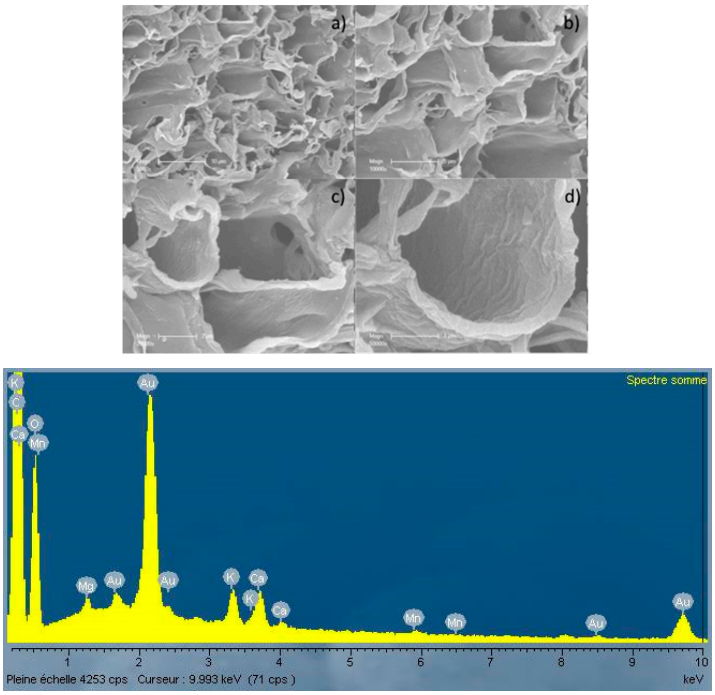

Figure 3. SEM photographs and X-ray fluorescence analysis of the surface of the biochar produced after pyrolysis of wood particles at 500 °C and different enlargements (**a**) ×5000; (**b**) ×10,000; (**c**) ×20,000; and (**d**) ×50,000.

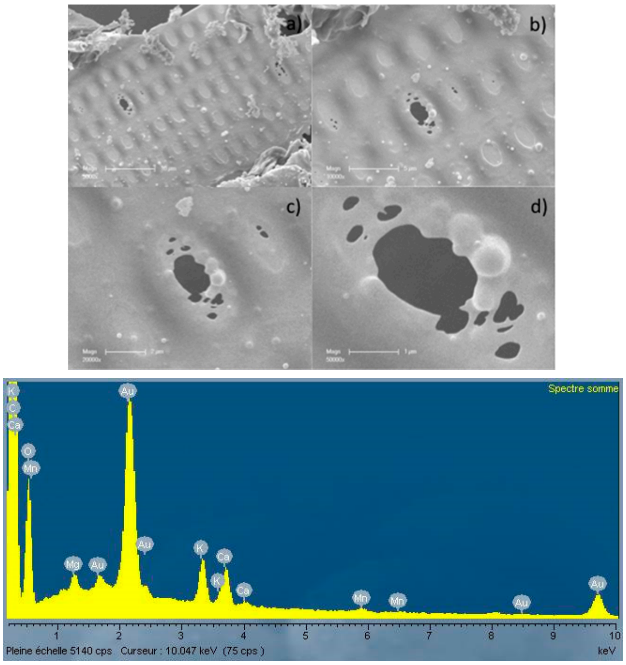

Figure 4. SEM photographs and X-ray fluorescence analysis of the surface of the biochar produced after pyrolysis of wood particles at 600 °C and different enlargements (**a**) ×5000; (**b**) ×10,000; (**c**) ×20,000; and (**d**) ×50,000.

The samples Char-500 and Char-600 present a smooth surface, comparable to the one of the raw biomass. They don't present any macropores (pores with diameter higher than 50 nm) and the shape of the particles remains identical to the raw biomass particles. The only difference is the concentrations of Ca and K, which increase with pyrolysis temperature (EDX spectra). The intensities of Ca and K peaks increase greatly with the pyrolysis temperature, bearing comparison to the principal Au peak (close to 2 keV). This phenomenon is due to the loss of volatile compounds from the raw biomass and then to the concentration of Ca and K. It also indicates that Ca and K are not completely emitted in the gas phase during the pyrolysis process when performed at 500 and 600 °C. Small amounts of Mg and Mn were observed in both samples.

Figures 5 and 6 show the surface of the chars obtained at 1200 and 1400 °C respectively. These photographs clearly show the modification of the particle surface shape at these temperatures due to sintering. At high enlargement (×50,000) small particles at the surface of the chars can be observed (Figures 4d and 5d). Analysis of the surface (EDX cartography—not shown) indicated that these particles contain only carbon, and no minerals. For the char obtained at 1200 °C, the amounts of Ca and K increased (with peak intensities comparable to that of Au) significantly, but the surface didn't present cracks or macropores (Figure 5d). Small amounts of Mg and Mn were also observed on these samples.

Figure 6a illustrates the deep modification of the biomass structure after a thermal treatment at 1400 °C. This sample is different from the others, with an important macro/mesoporosity appearing at the surface of the carbon residue (Figure 6d). This modification is also correlated with a decrease of the K content. As can be observed from the EDX analysis presented in Figure 6, the relative intensity of the K peak decreased significantly. This behavior can be explained by the sublimation/boiling of potassium during pyrolysis performed at 1400 °C (boiling point 1420 °C, sublimation at 1500 °C), leading to the appearance of large porosity at the surface of the char particle, or again to the char gasification by H_2O/CO_2 formed during the pyrolysis stage. This is consistent with other results obtained under similar conditions [23], which also showed that potassium released from char at 1400 °C was incorporated into soot particles.

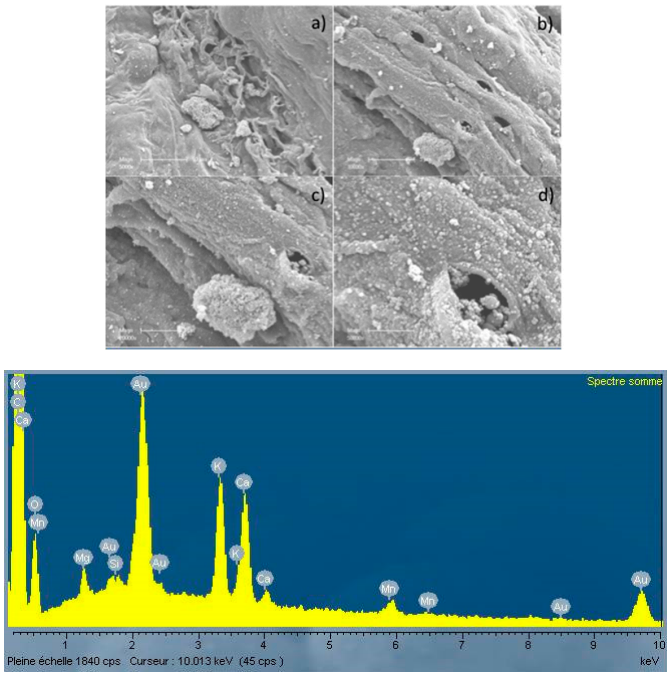

Figure 5. SEM photographs and X-ray fluorescence analysis of the surface of the biochar produced after pyrolysis of wood particles at 1200 °C and different enlargements (**a**) ×5000; (**b**) ×10,000; (**c**) ×20,000; and (**d**) ×50,000.

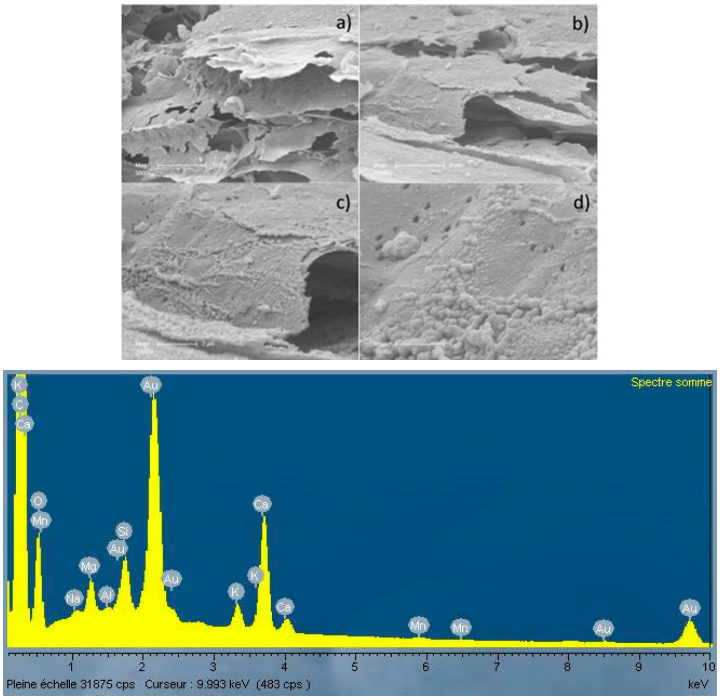

Figure 6. SEM photographs and X-ray fluorescence analysis of the surface of the biochar produced after pyrolysis of wood particles at 1400 °C and different enlargements (**a**) ×5000; (**b**) ×10,000; (**c**) ×20,000; and (**d**) ×50,000.

3.3. Chemical Composition

The chemical composition of the char samples is given in the Table 3. It shows that the char gets richer in C and poorer in H and O as the pyrolysis temperature increases. The C content increased from 47.1 mol % for the char-500 to 84 mol % for the char-1400. This enrichment in C with increasing temperature is well known in the literature. The O and H contents decreased significantly from 15.4 mol % and 37.5 mol % to 6.2 mol % and 9.9 mol % for the char-500 and the char-1400, respectively. Controlling the chemical composition of chars is relevant to many applications, such as tar removal, which was seen to depend on the C content of chars prepared by pyrolysis of rice husks [26].

Also, the C content of the char was seen to be related to the stability of the char in the soil when focusing on applications aiming at improving the soil quality or sequestrating the C for global warming mitigation [27].

Table 3. C, H and O contents of the different chars.

Sample	C [mol % afb]	H [mol % afb]	O [mol % afb]
char-500	47.1 ± 2.3	37.5 ± 0.8	15.4 ± 1.5
char-550	56.1 ± 1.3	32.4 ± 0.8	11.6 ± 0.5
char-600	63.4 ± 2.7	26.8 ± 1.1	9.9 ± 1.5
char-800	64.2 ± 1.5	26.9 ± 0.9	8.9 ± 0.6
char-1000	74.4 ± 3.1	15.0 ± 0.2	10.6 ± 2.8
char-1200	77.6 ± 2.6	14.0 ± 0.3	8.3 ± 2.2
char-1400	84.0 ± 2.7	9.9 ± 0.3	6.2 ± 2.4

3.4. FTIR Spectroscopy

FTIR spectra of the fresh wood and pyrolysis chars are shown in Figure 7. The wavenumber range is divided into two sub-ranges for the sake of clarity. The FTIR spectra of the unheated wood sample consist mainly of bands that can be attributed to carbohydrates (cellulose and hemicellulose)

and lignin. The most prominent carbohydrate bands in the raw wood can be found between 1000 and 1200 cm^{-1}, while those related to lignins were identified at approximately 1221, 1269, 1326, 1367, 1423, 1464, 1510 and 1596 cm^{-1} [11].

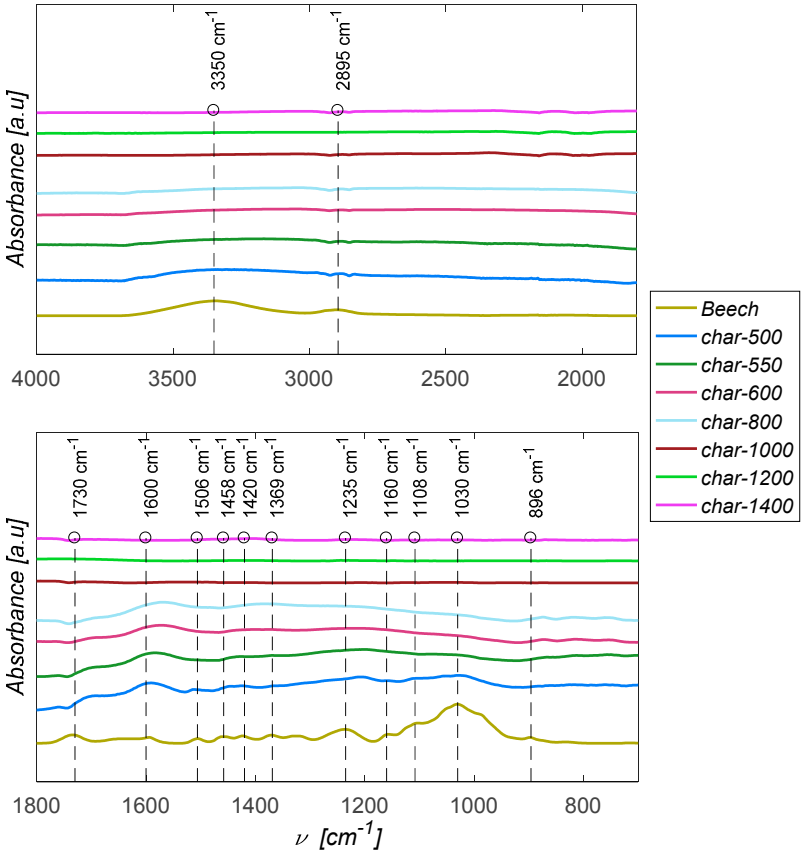

Figure 7. FTIR spectra of the pyrolysis solid residues.

Noticeable changes can be observed in the spectra of the chars compared to the raw wood. The OH band (around 3350 cm^{-1}) decreased significantly, starting with the char-500. The peak at 1730 cm^{-1}, related to the presence of carbonyl groups of esters and uronic acids in the xylan of beech wood progressively disappears as temperature increases. These functions belong to the hemicelluloses of beech wood, which have the lowest thermal stability [19].

Moreover, the two small peaks at 1506 and 1458 cm^{-1}, which are related to the Guaiacyl and Syringyl units of the beech wood lignin, are much less pronounced in char-500 than in raw beech, and completely vanish for the char-550 and beyond, confirming the high pyrolysis extent for this experiment. The peak at 1369 cm^{-1} is probably related to the C-H deformation in cellulose and hemicelluloses. This peak is only visible in raw beech, and no more in chars. The signal between 1000 and 1200 cm^{-1} is probably imputable to C-O vibrations in cellulose/hemicelluloses. It shows a high decrease for the char-500 confirming a high cellulose/hemicelluloses pyrolysis extent for this experiment. The signal vanishes completely for the char-550.

As stated previously, from 550 °C, the pyrolysis is nearly completed, which is reflected in the closeness of the char-550, char-600 and char-800 spectra. Beyond 800 °C, the signal intensity is very low through the infrared region of analysis. This denotes a much lower proportion of functional groups on the char surface, which is in agreement with the results of the elemental analysis.

3.5. Structural Changes of the Biomass Particles as Revealed by Raman Spectroscopy

The Raman spectra of the different chars are shown in Figure 8. The spectra are normalized according to the G band height. Raman spectra of amorphous biomass chars are known to exhibit two main peaks around 1350–1370 cm^{-1} and 1580–1600 cm^{-1}, commonly called the D and G bands.

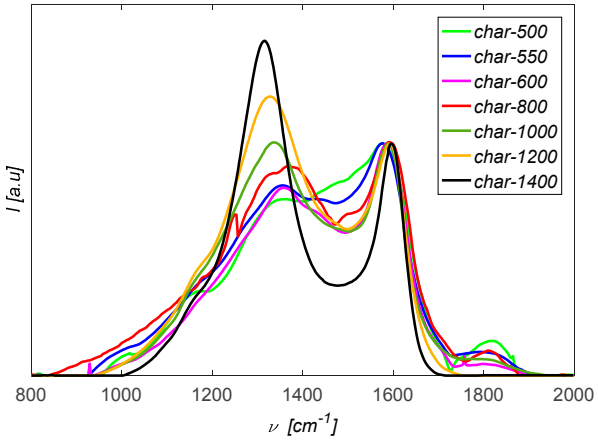

Figure 8. Raman spectra of the pyrolysis solid residues.

Increasing the pyrolysis temperature strongly affects the char structure. When increasing the temperature, Raman bands of pyrolysis residues appear as two overlapping but distinguishable peaks at the positions of approximately 1350 and 1600 cm^{-1}, which correspond to the in-plane vibrations of sp^2 -bonded carbon with structural defects D band and the in-plane vibrations of the sp^2-bonded graphitic carbon structures G band, respectively [26]. If a high proportion of amorphous carbon structures is present—which is the case for biomass chars—these two bands overlap. This overlapping is associated with hydrogen- and oxygen-rich amorphous carbon structures in the samples. This region (between 1400 and 1550 cm^{-1}) is called the valley region "V" [15].

Structural parameters such as the band intensity ratios $\frac{ID}{IG}$, $\frac{IV}{IG}$ or $\frac{IV}{ID}$ are indicators of the char structure. IV represents the valley intensity (taken as the minimum signal intensity between the D and G bands).

These structural parameters are summarized in Table 4. The D band position shifts to lower wavenumbers as pyrolysis temperature increases (from 1363 cm^{-1} at 500 °C to 1327 cm^{-1} at 1400 °C), while the G band position shifts to higher wavenumbers when increasing the pyrolysis temperature (from 1576 cm^{-1} at 500 °C to 1596 cm^{-1} at 1400 °C). This tendency was also observed previously during the characterization of chars prepared by cellulose slow pyrolysis at different temperatures [28]. This "red shift" in the D band peak position is more pronounced for low temperature chars, which have the highest contents of oxygenated defects structures [29].

Table 4. Evolution of the Total Raman Area (TRA), D and G band position as well as intensity ratios as a function of the pyrolysis reactor temperature.

Sample	*TRA*	Dposition [cm^{-1}]	Gposition [cm^{-1}]	$\frac{ID}{IG}$	$\frac{IV}{IG}$	$\frac{IV}{ID}$
char-500	410.87 ± 10.23	1363 ± 4	1576 ± 7	0.76 ± 0.05	0.82 ± 0.05	1.08 ± 0.04
char-550	418.53 ± 8.01	1351 ± 5	1576 ± 5	0.82 ± 0.03	0.74 ± 0.05	0.91 ± 0.05
char-600	368.25 ± 12.67	1357 ± 5	1588 ± 6	0.81 ± 0.07	0.65 ± 0.05	0.80 ± 0.03
char-800	438.93 ± 15.86	1366 ± 6	1599 ± 8	0.90 ± 0.08	0.62 ± 0.05	0.69 ± 0.07
char-1000	411.66 ± 14.34	1336 ± 5	1588 ± 6	1.01 ± 0.05	0.62 ± 0.05	0.62 ± 0.05
char-1200	362.75 ± 16.22	1326 ± 6	1590 ± 8	1.20 ± 0.06	0.63 ± 0.05	0.53 ± 0.05
char-1400	254.78 ± 12.35	1327 ± 7	1596 ± 4	1.44 ± 0.04	0.39 ± 0.05	0.27 ± 0.03

Furthermore, the intensity in the wavenumber ranges of 800 to 1100 cm^{-1} and 1700 to 1900 cm^{-1} strongly decreases with increasing pyrolysis temperature. This is related to the decrease of the highly reactive structures such as cycloheptane- and cyclooctane-centered ring systems, defective cyclic clusters and aromatic rings with pyrene sizes in the region of 800 to 1100 cm^{-1}, and to the pyrolysis of carbonyl bearing structures in the region of 1700 to 1900 cm^{-1} [30]. The decrease of the Raman signal in these regions (together with the valley region which is related to the amorphous carbon structures) is reflected in a decrease of the TRA with temperature, which was also denoted in [16] for cane trash chars, in [30] for mallee wood chars, as well as in [31] for miscanthus chars.

The Raman analysis also shows that the IV/IG ratio decreases sharply between 500 °C and 600 °C (from 0.82 to 0.65), reaches a plateau between 600 °C and 1200 °C, and then decreases sharply between 1200 °C and 1400 °C to reach 0.4. At 1400 °C, the thermal treatment must have been very severe to induce such a brutal change, indicating a probable graphitization in such conditions. McDonald-Wharry et al. [15] observed that the IV/IG height ratios level out at values approaching 0.4 for heat treatment between 700 and 1000 °C. However, the authors used different heat treatment conditions, with a much lower heating rate (7–30 °C/min) and a dwell/hold time of 20 min. Afterwards, the char was allowed to cool in an inert atmosphere to the ambient temperature. The authors think that this value obtained for IV/IG height ratios likely represents the overlap of broad D and G bands in the valley, and may not represent any amorphous carbon content, as might be the case for severe heat treatment.

The ratio $\frac{IV}{ID}$ decreases from 1.08 for the char-500 to 0.27 for the char-1400 which an ordering of the char structure. Moreover, the ID/IG ratio significantly increases with the pyrolysis temperature (from 0.76 at 500 °C to 1.44 at 1400 °C), indicating a higher proportion of condensed aromatic ring structures with defects. These D structures would be formed by the condensation of small aromatic amorphous carbon structures (valley region which intensity highly decreased with temperature). These results are in accordance with the dynamic molecular structure diagram established by Keiluweit et al. [10].

Altogether, an increasing level of order can be noticed in the structure of the char as the pyrolysis temperature increases, with a clearly distinguishable evolution of the Raman spectra of the different chars, especially for the 1400-char sample, the structure of which seems to be highly modified and ordered.

3.6. Char Reactivity towards O_2

The reactivities of chars towards O_2 were examined using thermogravimetric analysis. The obtained results are shown in Figure 9. Plots of the normalized mass ($\frac{m}{m_0} = f(T)$) and negative mass loss rate ($-\frac{dm}{dt} = f(T)$) are presented for raw beech wood and the different prepared chars.

Considering the experiment done on beech wood as reference, the mass loss below 300 °C decreases as pyrolysis temperature increases, indicating lower proportions of low, thermally stable components (reactive carbonaceous structure, incompletely pyrolysed wood) in the chars. The chars prepared at 500 °C and 550 °C (to a lower extent) show peaks (a maximum of degradation rate) at a relatively low temperature of 325 °C, probably indicating the presence of unconverted wood. The final residual mass increases with pyrolysis temperature, which was foreseeable, given that char obtained at higher temperatures has higher mineral content.

The char oxidation characteristics, defined previously in the materials and methods section, are summarized in Table 5. Char-600 unexpectedly shows higher thermal stability compared with char-800 and char-1000. In fact, the temperature corresponding to 50% of conversion is slightly higher for char-600 (405 °C) than for char-800 (379 °C) or char-1000 (389.4 °C). The prolonged char residence time in the reactor after pyrolysis has probably contributes to the thermal stability enhancement. Such behavior is confirmed by examination of the Raman spectra of the different samples. In fact, analysis of the Raman Spectra shows that char-600 has a lower intensity in the regions between 800 and

1200 cm^{-1} and 1700–1900 cm^{-1} when compared to the samples of char-800 and char-1000, respectively. Raman signal in these regions can be associated with the highly reactive structure in the char [29].

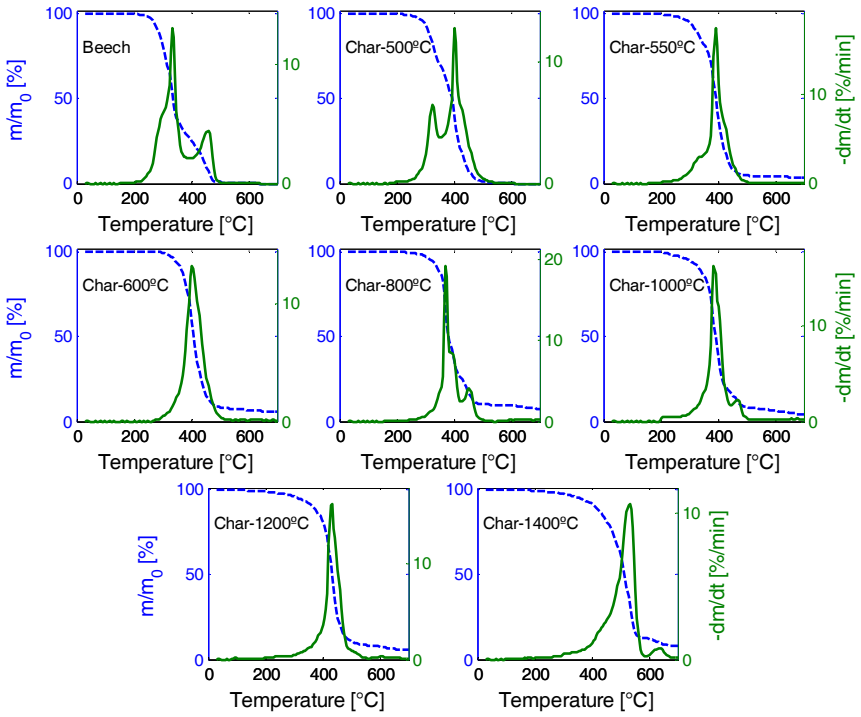

Figure 9. Normalized mass as a function of the temperature in the TG air oxidation experiments of the pyrolysis chars.

As shown in Figure 10, although the evolution of $T_{(50\%)}$ is somewhat chaotic between 500 °C and 1000 °C, it increases following a perfect linear relation (R^2 = 0.9999) with the char yield for the chars obtained between 1000 °C and 1400 °C. This could be linked to structural ordering and graphitization above 1000 °C.

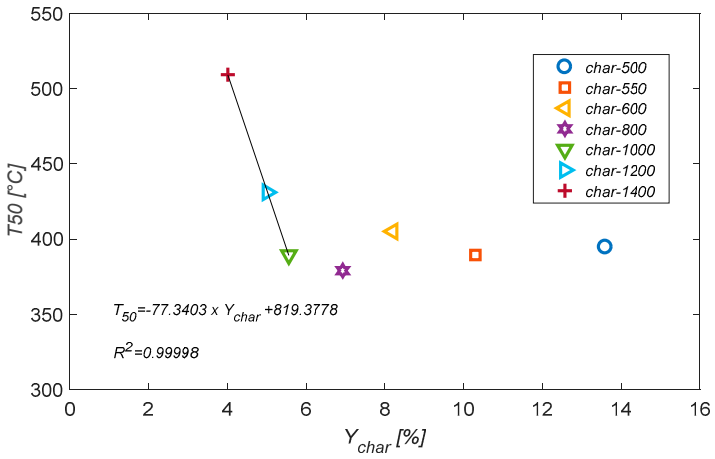

Figure 10. Evolution of $T_{50\%}$ with the char yield.

Moreover, the char mean reactivity significantly decreases as pyrolysis temperature increases, going from 0.198 min^{-1} for the char-500 to 0.067 min^{-1} for the char-1400, which represents nearly a threefold decrease.

The reactivity of fast pyrolysis beech bark and beech stick chars obtained between 450 °C and 850 °C were shown to be highly dependent on the pyrolysis temperature [20]. The authors think that at low pyrolysis temperatures, the high H and O contents of the char are associated with the presence of amorphous carbon structures and active sites that increase the char reactivity; whereas, when raising the pyrolysis temperature, the char reactivity decreases due the formation of more aromatic, less functionalized and less reactive structures.

We looked for possible relationships between the different reactivity parameters and the content of heteroatoms in the char (H and O). As shown in Figure 11, we found, for instance, that the mean reaction rate $-\frac{dm}{dt}_{mean}$ is linearly correlated with the O/C ratio. This linear dependence clearly expresses the influence of the surface functional groups containing O atoms on the char oxidation reaction rate.

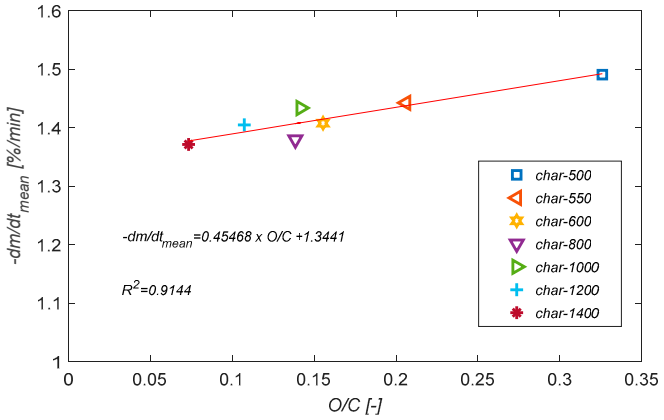

Figure 11. Mean mass loss rate of the char in the TG air oxidation experiments as a function of O/C atomic ratio.

Table 5 indicates that Char-1400 clearly presents the highest thermal stability and the lowest reactivity. In particular, Char-1400 has the lowest values for R_{mean} and R_{index} compared to the other samples. This thermal behavior may be linked to a more ordered carbonaceous structure [32], as revealed by the Raman spectroscopy analysis and reflected in the values of ID/IG and IV/IG, which were the highest and lowest, respectively, among all the samples, as well as representing the lowest $\left(\frac{O+H}{C}\right)$ atomic ratio.

Table 5. Characteristics of the char TG oxidation experiments.

Sample	$T_{(2\%)}$ [°C]	$T_{(50\%)}$ [°C]	$T_{(98\%)}$ [°C]	$T_{(-\frac{dm}{dt}\ max)}$ [°C]	$-\frac{dm}{dt}\ max$ [%/min]	$-\frac{dm}{dt}\ mean$ [%/min]	R_{mean} [min^{-1}]	R_{Index} [min^{-1}]
Beech	254.0	337.3	472.7	332.1	12.86	1.488	0.196	0.0216
char-500	269.6	394.6	488.3	399.8	17.53	1.488	0.198	0.0191
char-550	264.4	389.4	483.1	389.4	13.31	1.440	0.142	0.0265
char-600	321.7	405.0	545.6	399.8	19.20	1.405	0.119	0.0198
char-800	285.2	379.0	613.3	368.5	16.27	1.378	0.074	0.0299
char-1000	243.5	389.4	623.8	384.2	16.35	1.430	0.077	0.0247
char-1200	238.3	431.0	597.7	431.0	10.62	1.402	0.074	0.0232
char-1400	280.0	509.2	639.4	530.0	12.86	1.369	0.067	0.0132

Moreover, $T_{(50\%)}$ is, remarkably, correlated to the TRA following a linear relation (Figure 12). This relationship, indicating that $T_{(50\%)}$ increases when TRA decreases, makes sense, as the decrease of TRA is mainly due to the decrease of the contribution of the most reactive carbon structures to the Raman signal (amorphous carbon forms in the valley region and highly reactive groups on the two sides of the Raman spectra), which are less present in the char when the pyrolysis treatment is more

severe. Other researchers found a linear correlation between $\frac{1}{T_{(50\%)}}$ and the 2490 cm^{-1} band width (second order region in the Raman spectra) for cellulose chars treated between 600 and 2600 °C [19], while others found a linear relationship between $T_{(20\%)}$ and the area ratio of the G band to the TRA [22].

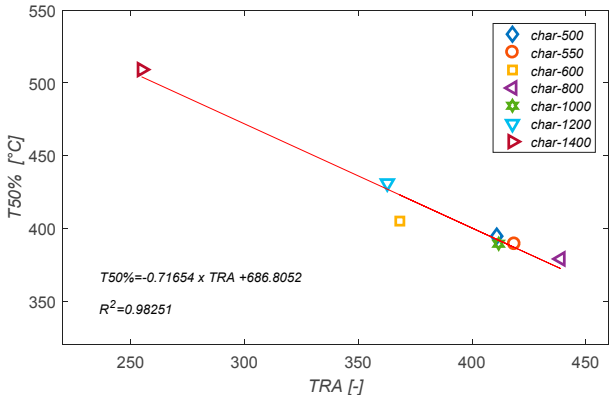

Figure 12. Evolution of $T_{(50\%)}$ with the TRA.

Reactivity index can also be correlated to the IV/ID structural ratio, as shown in Figure 13. This evolution here again makes sense, as the more reactive and amorphous small aromatic structures char contains, compared to condensed structures, the higher its reactivity.

Altogether, these oxidation reactivity tests show that the more severe the thermal treatment in the EFR is, the lower the reactivity of the char samples towards O_2 will be. The char reactivity, defined through several parameters, is also found to be remarkably correlated with many characteristics of the chars related to their structure and chemical composition.

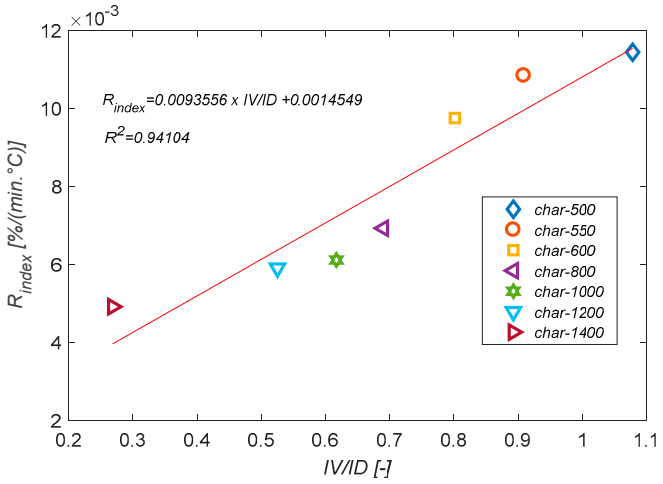

Figure 13. Evolution of $R_{(index)}$ with $\frac{\mathrm{IV}}{\mathrm{ID}}$.

4. Conclusions

This study examined the influence of biomass entrained flow pyrolysis conditions on the char properties. It was shown that the pyrolysis reactor temperature highly affects the char yield and properties in terms of morphology, surface chemistry, structure and reactivity. The char yield drops substantially from 14% to 4% when increasing the reactor temperature from 500 °C to 1400 °C. The surface chemistry became poor in surface functional groups beyond 800 °C. The morphology of the chars was highly modified at high temperature with a loss of the initial wood cell architecture, sintering, and macropore formation. Ca was seen to remain on the char while K highly devolatilizes at

1400 °C. Raman analyses showed an increasing ordering of the carbonaceous structures as temperature increases, with a higher content of condensed aromatic structures together with vanishing of the amorphous ones. The char reactivity expressed by means of various parameters equally changed with the pyrolysis temperature. For instance, the mean reactivity decreased nearly threefold for the char-1400 compared to the char-500. Several correlations between reactivity parameters, such as $\frac{dm}{dt}_{mean}$, $T_{(50\%)}$ and R_{index}, were seen to be correlated with O/C, TRA and IV/ID, respectively, which evidenced intimate relationships between chemical composition, structure and reactivity. These characterizations also reveal that it is possible to tailor the char properties according to the desired application by controlling the temperature and the particle residence time in an EFR. These two parameters should have the highest impact on the final char properties. We are currently working to further correlate the char properties of these two parameters and to measure their impacts on specific char physical and chemical characteristics.

Acknowledgments: The authors thank Jospeh Billaud for providing the char samples (800–1400 °C). They also thank Khouloud Haddad for her help in the acquisition of the Raman spectra.

Author Contributions: All authors contributed equally to the work done.

Conflicts of Interest: The authors declare no conflict of interest.

References

1. Markovska, N.; Duić, N.; Vad Mathiesen, B.; Guzović, Z.; Piacentino, A.; Schlör, H.; Lund, H. Addressing the main challenges of energy security in the twenty-first century—Contributions of the conferences on Sustainable Development of Energy, Water and Environment Systems. *Energy* **2016**, *115*, 1504–1512. [CrossRef]
2. Arodudu, O.; Helming, K.; Wiggering, H.; Voinov, A. Bioenergy from low-intensity agricultural systems: An energy efficiency analysis. *Energies* **2017**, *10*, 29. [CrossRef]
3. Chiodo, V.; Zafarana, G.; Maisano, S.; Freni, S.; Urbani, F. Pyrolysis of different biomass: Direct comparison among Posidonia Oceanica, Lacustrine Alga and White-Pine. *Fuel* **2016**, *164*, 220–227. [CrossRef]
4. No, S.-Y. Application of bio-oils from lignocellulosic biomass to transportation, heat and power generation—A review. *Renew. Sustain. Energy Rev.* **2014**, *40*, 1108–1125. [CrossRef]
5. Guizani, C.; Escudero Sanz, F.J.; Salvador, S. Influence of temperature and particle size on the single and mixed atmosphere gasification of biomass char with H_2O and CO_2. *Fuel Process. Technol.* **2015**, *134*, 175–188. [CrossRef]
6. Belhachemi, M.; Jeguirim, M.; Limousy, L.; Addoun, F. Comparison of NO_2 removal using date pits activated carbon and modified commercialized activated carbon via different preparation methods: Effect of porosity and surface chemistry. *Chem. Eng. J.* **2014**, *253*, 121–129. [CrossRef]
7. Zhu, L.; Shi, T.; Chen, Y. Preparation and characteristics of graphene oxide from the biomass carbon material using fir powder as precursor. *Fuller. Nanotub. Carbon Nanostruct.* **2015**, *23*, 961–967. [CrossRef]
8. Lehmann, J.; Joseph, S. *Biochar for Environmental Management: An Introduction*; Routledge: Abingdon, UK, 2009; pp. 1–14.
9. Brassard, P.; Godbout, S.; Raghavan, V.; Palacios, J.H.; Grenier, M.; Zegan, D. The production of engineered biochars in a vertical auger pyrolysis reactor for carbon sequestration. *Energies* **2017**, *10*, 288. [CrossRef]
10. Keiluweit, M.; Nico, P.S.; Johnson, M.; Kleber, M. Dynamic molecular structure of plant biomass-derived black carbon (biochar). *Environ. Sci. Technol.* **2010**, *44*, 1247–1253. [CrossRef] [PubMed]
11. Rutherford, D.W.; Wershaw, R.L.; Cox, L.G. *Changes in Composition and Porosity Occurring During the Thermal Degradation of Wood and Wood Components*; Scientific Investigations Report 2004-5292; United States Geological Survey: Reston, WV, USA, 2004.
12. Azargohar, R.; Nanda, S.; Kozinski, J.A.; Dalai, A.K.; Sutarto, R. Effects of temperature on the physicochemical characteristics of fast pyrolysis bio-chars derived from Canadian waste biomass. *Fuel* **2014**, *125*, 90–100. [CrossRef]
13. Guerrero, M.; Ruiz, M.P.; Alzueta, M.U.; Bilbao, R.; Millera, A. Pyrolysis of eucalyptus at different heating rates: Studies of char characterization and oxidative reactivity. *J. Anal. Appl. Pyrolysis* **2005**, *74*, 307–314. [CrossRef]

14. Rollinson, A.N. Gasifier reactor engineering approach to understanding the formation of biochar properties. *Proc. A R. Soc.* **2016**, *472*. [CrossRef] [PubMed]
15. McDonald-Wharry, J.; Manley-Harris, M.; Pickering, K. Carbonisation of biomass-derived chars and the thermal reduction of a graphene oxide sample studied using Raman spectroscopy. *Carbon* **2013**, *59*, 383–405. [CrossRef]
16. Keown, D.M.; Li, X.; Hayashi, J.I.; Li, C.Z. Characterization of the structural features of char from the pyrolysis of cane trash using Fourier transform-Raman spectroscopy. *Energy Fuels* **2007**, *21*, 1816–1821. [CrossRef]
17. Guizani, C.; Haddad, K.; Limousy, L.; Jeguirim, M. Document New insights on the structural evolution of biomass char upon pyrolysis as revealed by the Raman spectroscopy and elemental analysis. *Carbon* **2017**, *119*, 519–521. [CrossRef]
18. Trubetskaya, A.; Jensen, P.A.; Jensen, A.D.; Steibel, M.; Spliethoff, H.; Glarborg, P. Influence of fast pyrolysis conditions on yield and structural transformation of biomass chars. *Fuel Process. Technol.* **2015**, *140*, 205–214. [CrossRef]
19. Brewer, C.E.; Schmidt-rohr, K.; Satrio, J.A.; Brown, R.C. Characterization of biochar from fast pyrolysis and gasification systems. *Environ. Prog. Sustain. Energy* **2009**, *28*, 386–396. [CrossRef]
20. Morin, M.; Pécate, S.; Hémati, M.; Kara, Y. Pyrolysis of biomass in a batch fluidized bed reactor: Effect of the pyrolysis conditions and the nature of the biomass on the physicochemical properties and the reactivity of char. *J. Anal. Appl. Pyrolysis* **2016**, *122*, 511–523. [CrossRef]
21. Zaida, A.; Bar-Ziv, E.; Radovic, L.R.; Lee, Y.-J. Further development of Raman Microprobe spectroscopy for characterization of char reactivity. *Proc. Combust. Inst.* **2007**, *31*, 1881–1887. [CrossRef]
22. Sheng, C. Char structure characterised by Raman spectroscopy and its correlations with combustion reactivity. *Fuel* **2007**, *86*, 2316–2324. [CrossRef]
23. Billaud, J.; Valin, S.; Peyrot, M.; Salvador, S. Influence of H_2O, CO_2 and O_2 addition on biomass gasification in entrained flow reactor conditions: Experiments and modelling. *Fuel* **2016**, *166*, 166–178. [CrossRef]
24. Chen, L. Fast Pyrolysis of Millimetric Wood Particles between 800 °C and 1000 °C. Ph.D. Thesis, Claude Bernard Lyon I, Villeurbanne, France, December 2009.
25. Billaud, J.; Valin, S.; Ratel, G.; Thiery, S.; Salvador, S. Biomass gasification between 800 and 1400 °C in the presence of O_2: Drop tube reactor experiments and simulation. *Chem. Eng. Trans.* **2014**, *37*, 163–168. [CrossRef]
26. Paethanom, A.; Yoshikawa, K. Influence of pyrolysis temperature on rice husk char characteristics and its tar adsorption capability. *Energies* **2012**, *5*, 4941–4951. [CrossRef]
27. Crombie, K.; Mašek, O.; Sohi, S.P.; Brownsort, P.; Cross, A. The effect of pyrolysis conditions on biochar stability as determined by three methods. *GCB Bioenergy* **2013**, *5*, 122–131. [CrossRef]
28. Guizani, C.; Valin, S.; Billaud, J.; Peyrot, M.; Salvador, S. Biomass fast pyrolysis in a drop tube reactor for bio oil production: Experiments and modeling. *Fuel* **2017**, in press.
29. Smith, M.W.; Dallmeyer, I.; Johnson, T.J.; Brauer, C.S.; McEwen, J.S.; Espinal, J.F.; Garcia-Perez, M. Structural analysis of char by Raman spectroscopy: Improving band assignments through computational calculations from first principles. *Carbon* **2016**, *100*, 678–692. [CrossRef]
30. Asadullah, M.; Zhang, S.; Li, C.Z. Evaluation of structural features of chars from pyrolysis of biomass of different particle sizes. *Fuel Process. Technol.* **2010**, *91*, 877–881. [CrossRef]
31. Elmay, Y.; Le Brech, Y.; Delmotte, L.; Dufour, A.; Brosse, N.; Gadiou, R. Characterization of miscanthus pyrolysis by DRIFTs, UV Raman spectroscopy and mass spectrometry. *J. Anal. Appl. Pyrolysis* **2015**, *113*, 402–411. [CrossRef]
32. Asadullah, M.; Zhang, S.; Min, Z.; Yimsiri, P.; Li, C.Z. Effects of biomass char structure on its gasification reactivity. *Bioresour. Technol.* **2010**, *101*, 7935–7943. [CrossRef] [PubMed]